Self-consistent projection operator approach to excitation spectra: Role of correlated wave function

Y. Kakehashi
Max-Planck-Institut für Physik komplexer Systeme, Nöthnitzer Strasse 38, D-01187 Dresden, Germany
and National Center for Theoretical Sciences, 101 Section 2 Kuang Fu Road, Hsinchu, Taiwan 300, Republic of China

P. Fulde
Max-Planck-Institut für Physik komplexer Systeme, Nöthnitzer Strasse 38, D-01187 Dresden, Germany
(Received 16 October 2003; revised manuscript received 10 August 2004; published 27 October 2004)

A recently proposed combination of a projection operator method with the coherent potential approximation for the computation of the excitation spectra of solids is further extended. In particular, the effect of electron correlations on the matrix elements of the self-energy are investigated. This is done with the help of a Gutzwiller-type variational wave function. Numerical calculations have been performed for a half-filled band of a hypercubic lattice in infinite dimensions. They show that for strong electron correlations the higher-order dynamical corrections in an renormalized perturbation expansion are screened except in the low-energy regime. This provides for a justification of earlier work, where a Hartree-Fock approximation with a cutoff parameter was used for the computation of the static matrix elements.

DOI: 10.1103/PhysRevB.70.155112 PACS number(s): 71.10.Fd, 71.30.+h, 71.10.Li

I. INTRODUCTION

Single-site approaches to electron correlations provide for a good starting point for the understanding of excitation spectra and phase diagrams from the weak to the strong Coulomb interaction limit.[1] As regards the metal-insulator transition, such a theory was first proposed by Hubbard. He derived self-consistent equations for the self-energy of strongly correlated electrons by an equation of motion method.[2,3] The electrons were shown to behave as in an alloy with a random potential and therefore one is usually referring to the coherent potential approximation (CPA) for that system of equations.[4–9] Gutzwiller[10,11] proposed a wave function with locally correlated electrons which contains variational parameters. Their determination is possible within the so-called Gutzwiller approximation. Brinkman and Rice[12] found within the same approximation a diverging effective mass at the metal-insulator transition.

During the last decade, the single-site theory has gained in importance because of its relation to the limit of infinite dimensions. Metzner and Vollhardt[13] developed a theory for that limit by keeping the bandwidth as a constant. They showed that the Gutzwiller approximation becomes exact in that limit. Müller-Hartmann[14] proved that the self-energy is independent of momentum in that limit, and derived a self-consistent equation for it. Subsequently, many investigators[15–19] developed techniques to solve that equation self-consistently and extended the approach to the dynamical mean-field theory (DMFT). One result obtained within the DMFT is that the Fermi liquid state is so robust that it remains valid until a metal-insulator transition takes place.

In the theory of magnetism single-site theories were developed in order to describe magnetism for metallic as well as insulating states.[20–22] Hubbard[21] and Hasegawa[22] established a theory of single-site spin fluctuations (SSF) by using an alloy analogy in functional-integral theory.[23–26] The present authors[27] proposed a variational method which adiabatically takes into account those correlations missed in the SSF theory. Kakehashi[28,29] proposed the dynamical CPA which fully takes into account the dynamical spin and charge fluctuations within the single-site approximation. Hirooka and Shimizu[30] extended the CPA for disordered alloys to the many-body case (the many-body CPA) by using temperature Green functions. The many-body CPA, the dynamical CPA, and the DMFT have recently been shown to be equivalent to each other,[31] so that the theories of magnetism and those of strongly correlated electron systems can be considered in a unified way within the single-site approximation.

Several of the theories mentioned above are based on temperature Green functions, but one may as well construct a single-site approximation for the retarded Green function. In particular, the projection operator method[32–34] has been used to formulate a single-site approximation in terms of the wave operator.[35–38] With the help of the method of increments[39] one should be able to go beyond that approximation and to account for the momentum dependence of the self-energy. Corresponding calculations for the ground state of semiconductors and insulators have led to very accurate results, i.e., ones of quantum chemical accuracy. For a review see Ref. 38. Reaching a similar accuracy for energy bands would open up the road toward a realistic description of the excitation spectra outside the standard approximations within density-functional theory. For that reason we have recently developed as a first step a single-site theory which combines the projection operator method with the CPA, i.e., the projection operator method CPA (PM-CPA).[40] It was worked out for a Hubbard Hamiltonian. The projection operator method describes the dynamics of single-particle excitations by means of a Liouville operator L. The PM-CPA self-consistently takes into account the effects of the dynamics of the environment of a given site by making a single-site approximation. This results in an energy dependent Liouville

operator $\tilde{L}(z)$. The latter is determined by the CPA equation. It requires that an impurity Green function embedded in an effective medium should be identical with the coherent Green function of the effective medium.

In order to solve the impurity problem we developed in the previous paper[40] a renormalized perturbation theory. It allows for determining the memory function of the retarded Green function by including more and more dynamical variables in the projected operator space. Within this expansion procedure a decoupling approximation was made.

The corresponding static matrix elements were evaluated by a Hartree-Fock approximation with a phenomenological cutoff parameter q. The latter was equal to 1 for the metallic and 0 for the insulating state. This way a satisfactory excitation spectrum was obtained for all interaction strengths, when the case of half filling was considered for a hypercubic lattice in infinite dimensions.

The use of the Hartree-Fock approximation for the matrix elements in the strongly correlated regime, however, cannot be justified in general. We need to examine the effects of electron correlations on the static matrix elements and hence on the excitation spectrum in more detail. In the present paper, we calculate various static matrix elements of the memory function with respect to the ground state by adopting for the latter a Gutzwiller-type variational wave function.[41] We clarify the role of local correlations on the excitation spectrum. In particular we will justify the phenomenological cutoff parameter introduced in our previous paper.[40]

In the following section, we briefly review the PM-CPA and summarize the self-consistent equations to be solved. In Sec. III, we calculate various static quantities that appear in the memory function. As mentioned above we apply for that purpose a Gutzwiller-type variational wave function.[41] The wave function that we use here describes best the local electron correlations for weak correlations, but also leads to the correct atomic limit for a half-filled band. A conventional single-site approximation to the static matrix elements does not lead to a Fermi-liquid behavior of the single-particle excitations. We treat this problem in Sec. III B, and obtain the memory function for correlated electrons in Sec. III C.

We present numerical results in Sec. IV for the excitation spectrum in infinite dimensions. The inclusion of electron correlations shows the development of the upper and lower Hubbard bands in the intermediate interaction regime. It is also found that the Hubbard bands are well described by the zeroth approximation in the renormalized perturbation scheme because of the screening of the higher-order terms. This justifies the Hartree-Fock approximation with a phenomenological cutoff parameter for the calculation of the static quantities. A summary is given and the remaining problems are discussed in the last Sec. V.

II. PROJECTION OPERATOR CPA

We adopt here the Hubbard Hamiltonian[10,2] with an intraatomic Coulomb interaction U:

$$H = H_0 + U\sum_i n_{i\uparrow}n_{i\downarrow}, \tag{1}$$

$$H_0 = \sum_{i,\sigma}(\epsilon_0 - \mu)n_{i\sigma} + \sum_{i,j,\sigma} t_{ij}a^\dagger_{i\sigma}a_{j\sigma}, \tag{2}$$

where ϵ_0 and t_{ij} are the atomic level and the transfer integral between sites i and j, respectively, and $a^\dagger_{i\sigma}$ ($a_{i\sigma}$) is a creation (annihilation) operator for an electron with spin σ on site i. Furthermore, $n_{i\sigma}=a^\dagger_{i\sigma}a_{i\sigma}$. μ is the chemical potential.

The single-particle excitation spectrum is obtained from the retarded Green function as[1]

$$G_{ij\sigma}(z) = \left\langle a^\dagger_{i\sigma}\left|\frac{1}{z-L}a^\dagger_{j\sigma}\right.\right\rangle, \tag{3}$$

where $z=\omega+i\delta$ with δ being an infinitesimal positive number. The Liouville operator L is a superoperator acting on an operator A as $LA=[H,A]_-$. The inner product between the operators A and B is defined by $(A|B)=\langle[A^+,B]_+\rangle$.

In the PM-CPA,[40] we approximate the Liouville operator by means of an energy dependent Liouville operator $\tilde{L}(z)$ for an effective Hamiltonian $\tilde{H}(z)$:

$$\tilde{H}(z) = H_0 + \sum_{i\sigma}\Sigma_\sigma(z)a^\dagger_{i\sigma}a_{i\sigma}. \tag{4}$$

Here $\Sigma_\sigma(z)$ is a site-diagonal self-energy called the coherent potential. The diagonal Green function to the Liouville operator $\tilde{L}(z)$, which we call the coherent Green function, is obtained as

$$F_\sigma(z) = \int \frac{\rho(\epsilon)d\epsilon}{z-\epsilon_0+\mu-\Sigma_\sigma(z)-\epsilon}, \tag{5}$$

where $\rho(\epsilon)$ is the density of states (DOS) per atom for the noninteracting system specified by t_{ij}.

The coherent potential introduced in Eq. (4) is determined self-consistently from the CPA condition that the impurity Green function embedded in the effective medium is identical with the coherent one, i.e.,

$$G^{(i)}_\sigma(z) = F_\sigma(z). \tag{6}$$

The impurity Green function is given by

$$G^{(i)}_\sigma(z) = [F_\sigma(z)^{-1} - \Lambda^{(i)}_\sigma(z) + \Sigma_\sigma(z)]^{-1}, \tag{7}$$

$$\Lambda^{(i)}_\sigma(z) = U\langle n_{i-\sigma}\rangle + U^2\overline{G}^{(i)}_\sigma(z). \tag{8}$$

The first term on the right-hand side (RHS) in Eq. (8) is the Hartree-Fock potential. The reduced memory function $\overline{G}^{(i)}_\sigma(z)$ in the second term is given by

$$\overline{G}^{(i)}_\sigma(z) = (A^\dagger_{i\sigma}|[z-\overline{L}^{(i)}(z)]^{-1}A^\dagger_{i\sigma}). \tag{9}$$

Here the operator $A^\dagger_{i\sigma}$ is defined by $A^\dagger_{i\sigma}=a^\dagger_{i\sigma}\delta n_{i-\sigma}$ and $\delta n_{i-\sigma}=n_{i-\sigma}-\langle n_{i-\sigma}\rangle$. The Liouville operator $\overline{L}^{(i)}(z)=QL^{(i)}(z)Q$ acts on a space that is orthogonal to $\{|a^\dagger_{j\sigma})\}$. This is achieved

through the projection operator $Q=1-P$, where $P=\Sigma_{j\sigma}|a_{j\sigma}^{\dagger})(a_{j\sigma}^{\dagger}|$. $L^{(i)}(z)$ is a Liouville operator for an impurity Hamiltonian $H^{(i)}(z)$ with a Coulomb interaction on site i embedded in the effective medium:

$$H^{(i)}(z) = \tilde{H}(z) - \sum_{\sigma} \Sigma_{\sigma}(z) a_{i\sigma}^{\dagger} a_{i\sigma} + U n_{i\uparrow} n_{i\downarrow}. \tag{10}$$

The memory function (9) is calculated by means of the renormalized perturbation theory (RPT) as[40]

$$\overline{G}_{\sigma}^{(i)}(z) = \frac{\overline{G}_{0\sigma}^{(i)}(z)}{1 - \overline{L}_{I\sigma}^{(i)}(z)\overline{G}_{0\sigma}^{(i)}(z)}, \tag{11}$$

$$\overline{L}_{I\sigma}^{(i)}(z) = \frac{-\Sigma_{\sigma}(z) + U(1-\langle n_{i-\sigma}\rangle)}{\langle n_{i-\sigma}\rangle(1-\langle n_{i-\sigma}\rangle)}. \tag{12}$$

$\overline{G}_{0\sigma}^{(i)}$ is a screened memory function defined by

$$\overline{G}_{0\sigma}^{(i)}(z) = (A_{i\sigma}^{\dagger}|[z - \overline{L}_0(z) - \overline{L}_I^{(i)}(z)\overline{Q}]^{-1}A_{i\sigma}^{\dagger}). \tag{13}$$

Here $\overline{L}_0(z) = Q\tilde{L}(z)Q$ and $\overline{L}_I^{(i)}(z) = QL_I^{(i)}(z)Q$. The Liouvillean $L_I^{(i)}(z)$ acts on a given operator A according to $L_I^{(i)}(z)A = [-\Sigma_{\sigma}\Sigma_{\sigma}(z)n_{i\sigma} + Un_{i\uparrow}n_{i\downarrow}, A]_-$. Moreover, $\overline{Q} = 1-\overline{P}$, $\overline{P} = \Sigma_{i\sigma}|A_{i\sigma}^{\dagger})\chi_{i\sigma}^{-1}(A_{i\sigma}^{\dagger}|$, and $\chi_{i\sigma} = \langle n_{i-\sigma}\rangle(1-\langle n_{i-\sigma}\rangle)$.

The RPT interpolates between the weak and strong Coulomb interaction limits. Note that the operator $\overline{L}_I^{(i)}(z)\overline{Q}$ in Eq. (13) is negligible in both limits. In the intermediate regime, we expand the screened memory function $\overline{G}_{0\sigma}^{(i)}(z)$ with respect to $\overline{L}_I^{(i)}(z)\overline{Q}$ up to the first order exactly. For the higher-order terms, we make use of a decoupling approximation within the operator space $\{|a_{k\sigma}^{\dagger}\delta(a_{k'-\sigma}^{\dagger}a_{k''-\sigma}))\}$. Here $a_{k\sigma}^{\dagger}$ $(a_{k\sigma})$ is the creation (annihilation) operator for an electron with momentum k and spin σ. This is called the first-order renormalized perturbation theory (the RPT-1).[40] We have then

$$\overline{G}_{0\sigma}^{(i)}(z) = [\overline{G}_{0\sigma}^{(i)}(z)]_0 + \frac{[\Delta\overline{G}_{0\sigma}^{(i)}(z)]_1}{1 - \overline{R}_{\sigma}^{(i)}(z)}. \tag{14}$$

The first term on the RHS of Eq. (14) is the zeroth expansion term (the RPT-0). $[\overline{G}_{0\sigma}^{(i)}(z)]_0$, $[\Delta\overline{G}_{0\sigma}^{(i)}(z)]_1$, and $\overline{R}_{\sigma}^{(i)}(z)$ are given as follows:

$$[\overline{G}_{0\sigma}^{(i)}(z)]_0 = \frac{1}{N^3}\sum_{k,k',k''} \frac{X_{\sigma}^{(0)}(\epsilon_k, \varepsilon_{k'}, \varepsilon_{k''})}{z - \tilde{\epsilon}_{\sigma} - \tilde{\Sigma}_{\sigma}(z) - \epsilon_k - \epsilon_{k'} + \epsilon_{k''}}, \tag{15}$$

$$[\Delta\overline{G}_{0\sigma}^{(i)}(z)]_1 = \frac{1}{N^3}\sum_{k,k',k''} \frac{X_{\sigma}^{(0)}(\epsilon_k, \epsilon_{k'}, \epsilon_{k''})\Delta_{\sigma}(z - \tilde{\epsilon}_{\sigma} - \tilde{\Sigma}_{\sigma}(z), \tilde{\Sigma}_{\sigma}(z), \epsilon_k, \epsilon_{k'}, \epsilon_{k''})}{z - \tilde{\epsilon}_{\sigma} - \tilde{\Sigma}_{\sigma}(z) - \epsilon_k - \varepsilon_{k'} + \varepsilon_{k''}}, \tag{16}$$

$$\overline{R}_{\sigma}^{(i)}(z) = \frac{1}{N^3}\sum_{k,k',k''} \Delta_{\sigma}(z - \tilde{\epsilon}_{\sigma} - \tilde{\Sigma}_{\sigma}(z), \tilde{\Sigma}_{\sigma}(z), \epsilon_k, \epsilon_{k'}, \epsilon_{k''}). \tag{17}$$

Here $\tilde{\epsilon}_{\sigma} = \epsilon_0 - \mu + U\langle n_{i-\sigma}\rangle$ and $\tilde{\Sigma}_{\sigma}(z) = \Sigma_{\sigma}(z) - U\langle n_{i-\sigma}\rangle$. N is the number of sites and ϵ_k is an eigenvalue of t_{ij} with momentum k.

The functions $X_{\sigma}^{(0)}(\epsilon_k, \epsilon_{k'}, \epsilon_{k''})$ and $\Delta_{\sigma}(z, \tilde{\Sigma}_{\sigma}(z), \epsilon_k, \epsilon_{k'}, \epsilon_{k''})$ in Eqs. (15)–(17) are given by

$$X_{\sigma}^{(0)}(\epsilon_k, \epsilon_{k'}, \epsilon_{k''}) = N^3 \sum_{k_1,k_1',k_1''} \langle i|k_1\rangle\langle i|k_1'\rangle\langle k_1''|i\rangle(\boldsymbol{\chi}_0)_{k_1k_1'k_1''\sigma k k' k''\sigma}\langle k|i\rangle\langle k'|i\rangle\langle i|k''\rangle, \tag{18}$$

$$\Delta_{\sigma}(z, \tilde{\Sigma}_{\sigma}(z), \epsilon_k, \epsilon_{k'}, \epsilon_{k''}) = N^3 \sum_{k_1,k_1',k_1''} \frac{\langle i|k\rangle\langle i|k'\rangle\langle k''|i\rangle[\mathbf{L}_{IQ}^{(i)}(z)]_{kk'k''\sigma k_1k_1'k_1''\sigma}\langle k_1|i\rangle\langle k_1'|i\rangle\langle i|k_1''\rangle}{z - \epsilon_{k_1} - \epsilon_{k_1'} + \epsilon_{k_1''}}. \tag{19}$$

Here $\langle k|i\rangle = \langle i|k\rangle^* = 1/\sqrt{N}\exp(i\mathbf{k}\cdot\mathbf{R}_i)$, and

$$(\mathbf{L}_{IQ}^{(i)})_{k_1k_1'k_1''\sigma kk'k''\sigma} = -\tilde{\Sigma}_\sigma(z)\langle i|k\rangle\langle k_1|i\rangle\delta_{k_1'k'}\delta_{k_1''k''} - \tilde{\Sigma}_{-\sigma}(z)\langle i|k'\rangle \times\langle k_1'|i\rangle\delta_{k_1k}\delta_{k_1''k''} + \tilde{\Sigma}_{-\sigma}(z)\langle k''|i\rangle \times\langle i|k_1''\rangle\delta_{k_1k}\delta_{k_1'k'} + U(\boldsymbol{\chi}_0^{-1}\mathbf{L}_U^{(i)})_{k_1k_1'k_1''\sigma kk'k''\sigma} - \overline{L_{I\sigma}^{(i)}}(z)\langle k_1|i\rangle\langle k_1'|i\rangle\langle i|k_1''\rangle \times(A_{i\sigma}^\dagger|a_{k\sigma}^\dagger\delta(a_{k'-\sigma}^\dagger a_{k''-\sigma})), \tag{20}$$

$$(\boldsymbol{\chi}_0)_{k_1k_1'k_1''\sigma kk'k''\sigma} = (a_{k_1\sigma}^\dagger\delta(a_{k_1'-\sigma}^\dagger a_{k_1''-\sigma})|a_{k\sigma}^\dagger\delta(a_{k'-\sigma}^\dagger a_{k''-\sigma})), \tag{21}$$

$$(\mathbf{L}_U^{(i)})_{k_1k_1'k_1''\sigma kk'k''\sigma} = (a_{k_1\sigma}^\dagger\delta(a_{k_1'-\sigma}^\dagger a_{k_1''-\sigma})|A_{i\sigma}^\dagger\delta(a_{k'-\sigma}^\dagger a_{k''-\sigma}))\langle i|k\rangle + (a_{k_1\sigma}^\dagger\delta(a_{k_1'-\sigma}^\dagger a_{k_1''-\sigma})|a_{k\sigma}^\dagger A_{i-\sigma}^\dagger a_{k''-\sigma})\langle i|k'\rangle - (a_{k_1\sigma}^\dagger\delta(a_{k_1'-\sigma}^\dagger a_{k_1''-\sigma})|a_{k\sigma}^\dagger a_{k'-\sigma}^\dagger A_{i-\sigma})\langle k''|i\rangle. \tag{22}$$

The functions $X_\sigma^{(0)}(\epsilon_k,\epsilon_{k'},\epsilon_{k''})$ and $\Delta_\sigma(z,\tilde{\Sigma}_\sigma(z),\epsilon_k,\epsilon_{k'},\epsilon_{k''})$ were obtained previously in the Hartree-Fock approximation as[40]

$$\chi_\sigma(\epsilon_k,\epsilon_{k'},\epsilon_{k''}) = f(-\epsilon_k-\tilde{\epsilon}_\sigma)f(-\epsilon_{k'}-\tilde{\epsilon}_{-\sigma})f(\epsilon_{k''}+\tilde{\epsilon}_{-\sigma}) + f(\epsilon_k+\tilde{\epsilon}_\sigma)f(\epsilon_{k'}+\tilde{\epsilon}_{-\sigma})f(-\epsilon_{k''}-\tilde{\epsilon}_{-\sigma}), \tag{23}$$

$$\Delta_\sigma^{(HF)}(z,\tilde{\Sigma}_\sigma(z),\epsilon,\epsilon',\epsilon'') = -\tilde{\Sigma}_\sigma(z)[\hat{F}(z-\epsilon'+\epsilon'') + \hat{F}(z-\epsilon+\epsilon'') + \hat{F}(-z+\epsilon+\epsilon')] + UK_\sigma(z,\epsilon',\epsilon'') - \overline{L_{I\sigma}^{(i)}}(z)\hat{\Sigma}_\sigma^{(2)}(z). \tag{24}$$

Here $f(\omega)$ is the Fermi distribution function. The functions $\hat{F}(z)$, $K_\sigma(z,\epsilon',\epsilon'')$, and $\hat{\Sigma}_\sigma^{(2)}(z)$ are defined by

$$\hat{F}(z) = \int\frac{\rho(\epsilon)d\epsilon}{z-\epsilon}, \tag{25}$$

$$K_\sigma(z,\epsilon',\epsilon'') = \int\frac{d\omega\,d\omega''\rho(\omega)\rho(\omega'')[f(\tilde{\epsilon}_\sigma+\omega)-f(\tilde{\epsilon}_{-\sigma}+\omega'')]}{z-\omega-\epsilon'+\omega''} + \int\frac{d\omega\,d\omega'\rho(\omega)\rho(\omega')[f(-\tilde{\epsilon}_{-\sigma}-\omega')-f(\tilde{\epsilon}_{-\sigma}+\omega)]}{z-\omega-\omega'+\epsilon''}, \tag{26}$$

$$\hat{\Sigma}_\sigma^{(2)}(z) = \int\frac{d\epsilon\,d\epsilon'd\epsilon''\rho(\epsilon)\rho(\epsilon')\rho(\epsilon'')\chi_\sigma(\epsilon,\epsilon',\epsilon'')}{z-\epsilon_k-\epsilon_{k'}+\epsilon_{k''}}. \tag{27}$$

Note that $U^2\hat{\Sigma}_\sigma^{(2)}(z)$ is the self-energy in second-order perturbation theory.

III. WAVE FUNCTION APPROACH TO THE STATIC MATRIX ELEMENTS

A. Weak-scattering approximation and wave function

In the first-order renormalized perturbation scheme, the effects of the static correlations appear only via $X_\sigma^{(0)}(\epsilon_k,\epsilon_{k'},\epsilon_{k''})$ and $\Delta_\sigma(z,\tilde{\Sigma}(z),\epsilon,\epsilon',\epsilon'')$ as seen from Eqs. (14)–(17). Since Δ_σ is related to higher-order terms in the expansion series, we approximate it in the following by the Hartree-Fock value $\Delta_\sigma^{(HF)}$, and introduce the renormalization constants A_σ and B_σ so that the correct zeroth order moment of Δ_σ is reproduced:

$$\Delta_\sigma(z,\tilde{\Sigma}(z),\epsilon,\epsilon',\epsilon'') = -\tilde{\Sigma}_\sigma(z)[\hat{F}(z-\epsilon'+\epsilon'') + \hat{F}(z-\epsilon+\epsilon'') + \hat{F}(-z+\epsilon+\epsilon')] + B_\sigma UK_\sigma(z,\epsilon',\epsilon'') - A_\sigma\overline{L_{I\sigma}^{(i)}}(z)\hat{\Sigma}_\sigma^{(2)}(z). \tag{28}$$

Here $A_\sigma=\langle n_{i-\sigma}\rangle(1-\langle n_{i-\sigma}\rangle)/\langle n_{i-\sigma}\rangle_0(1-\langle n_{i-\sigma}\rangle_0)$, $B_\sigma=(1-2\langle n_{i-\sigma}\rangle)/(1-2\langle n_{i-\sigma}\rangle_0)$, and $\langle\ \rangle_0$ denotes the Hartree-Fock average.

Equation (28) is a weak-scattering approximation, and correlation effects on $\overline{G_{0\sigma}^{(i)}}(z)$ are linearized because both $[\overline{G_{0\sigma}^{(i)}}(z)]_0$ and $[\Delta\overline{G_{0\sigma}^{(i)}}(z)]_1$ depend linearly on the remaining correlation term $X_\sigma^{(0)}(\epsilon_k,\epsilon_{k'},\epsilon_{k''})$.

For the calculation of $X_\sigma^{(0)}(\epsilon_k,\epsilon_{k'},\epsilon_{k''})$ defined by Eq. (18), we consider the ground state and adopt a variational wave function Ψ of the Gutzwiller-type[41]

$$|\Psi\rangle = \prod_i(1-\eta_iO_i)|\phi_0\rangle. \tag{29}$$

Here $|\phi_0\rangle$ denotes the Hartree-Fock wave function. The local operator $O_i=\delta n_{i\uparrow}\delta n_{i\downarrow}$ describes local electron correlations on site i, and the $\{\eta_i\}$ are variational parameters. The wave function describes best the on-site correlations from the weak to the intermediate Coulomb interaction regime. For a half-filled band it leads to the correct atomic limit.

The variational parameter η_i is determined from the stationary condition to the ground state energy $\partial\langle H\rangle/\partial\eta_i=0$. In the single-site approximation, it is given by

$$\eta_i = \frac{-\langle O_i\tilde{H}O_i\rangle_0 + \sqrt{\langle O_i\tilde{H}O_i\rangle_0^2 + 4\langle O_i\tilde{H}\rangle_0\langle O_i^2\rangle_0}}{2\langle O_i\tilde{H}\rangle_0\langle O_i^2\rangle_0}, \tag{30}$$

and the average value of an operator A is given by

$$\langle A\rangle = \langle A\rangle_0 + \sum_i\frac{-\eta_i(\langle O_i\tilde{A}\rangle_0 + \langle\tilde{A}O_i\rangle_0) + \eta_i^2\langle O_i\tilde{A}O_i\rangle_0}{1+\eta_i^2\langle O_i^2\rangle_0}. \tag{31}$$

Here $\tilde{A}=A-\langle A\rangle_0$ and $\langle O_i^2\rangle_0=\langle n_{i\uparrow}\rangle_0[1-\langle n_{i\uparrow}\rangle_0]\langle n_{i\downarrow}\rangle_0[1-\langle n_{i\downarrow}\rangle_0]$.

We apply the above formula to the calculation of $X_\sigma^{(0)}(\epsilon_k,\epsilon_{k'},\epsilon_{k''})$ given by Eq. (18). For that purpose, we express $\boldsymbol{\chi}_0$ as a thermal average instead of an inner product. Adopting Eq. (31), we obtain

$$X^{(0)}(\epsilon_k,\epsilon_{k'},\epsilon_{k''}) = \chi(\epsilon_k,\epsilon_{k'},\epsilon_{k''}) - \frac{\eta}{1+\eta^2\langle O_i^2\rangle_0}X_1(\epsilon_k,\epsilon_{k'},\epsilon_{k''}) + \frac{\eta^2}{1+\eta^2\langle O_i^2\rangle_0}X_2(\epsilon_k,\epsilon_{k'},\epsilon_{k''}). \quad (32)$$

Here and in the following we consider the half-filled band for a nonmagnetic state, and omit the spin index σ for brevity. Then $X_1(\epsilon_k,\epsilon_{k'},\epsilon_{k''})$ and $X_2(\epsilon_k,\epsilon_{k'},\epsilon_{k''})$ are given by

$$\begin{aligned} X_1(\epsilon_k,\epsilon_{k'},\epsilon_{k''}) &= -\frac{1}{N}\sum_K\sum_{k_1k_1'}\delta_{-k+k_1-k_1'+k'',K}[f(\epsilon_{k''})f(-\epsilon_{k_1'})f(\epsilon_{k_1})f(-\epsilon_k) \\ &\quad + f(-\epsilon_{k''})f(\epsilon_{k_1'})f(-\epsilon_{k_1})f(\epsilon_k)] \\ &\quad + \frac{1}{N}\sum_K\sum_{k_1k_1'}\delta_{-k+k_1-k'+k_1',K}[f(\epsilon_{k_1'})f(-\epsilon_{k'})f(\epsilon_{k_1})f(-\epsilon_k) \\ &\quad + f(-\epsilon_{k_1'})f(\epsilon_{k'})f(-\epsilon_{k_1})f(\epsilon_k)], \end{aligned} \quad (33)$$

$$\begin{aligned} X_2(\epsilon_k,\epsilon_{k'},\epsilon_{k''}) &= \frac{1}{4N}\sum_K\sum_{k_1k_1'}\delta_{-k'+k_1-k_1'+k'',K}[f(\epsilon_{k''})-f(\epsilon_{k_1})][f(\epsilon_{k_1'})-f(\epsilon_{k'})] \\ &\quad - \frac{1}{4N}\sum_K\sum_{k_1k_1'}\delta_{-k+k_1-k_1'+k'',K}[f(\epsilon_{k_1})f(\epsilon_k)-f(-\epsilon_{k_1})f(-\epsilon_k)][f(\epsilon_{k_1'})f(\epsilon_{k''})-f(-\epsilon_{k_1'})f(-\epsilon_{k''})] \\ &\quad + \frac{1}{4N}\sum_K\sum_{k_1k_1'}\delta_{-k+k_1-k'+k_1',K}[f(\epsilon_{k_1})f(\epsilon_k)-f(-\epsilon_{k_1})f(-\epsilon_k)][f(\epsilon_{k_1'})f(\epsilon_{k'})-f(-\epsilon_{k_1'})f(-\epsilon_{k'})] \\ &\quad + \frac{1}{8}\{[f(\epsilon_k)-f(\epsilon_{k''})][f(-\epsilon_{k'})-f(\epsilon_{k'})]+[f(-\epsilon_k)-f(\epsilon_{k'})][f(-\epsilon_{k''})-f(\epsilon_{k''})]+[f(\epsilon_{k''})-f(\epsilon_{k'})][f(\epsilon_k)-f(-\epsilon_k)]\}. \end{aligned} \quad (34)$$

Here K denotes the reciprocal lattice vector of the system.

B. Two-point approximation to the static average

The expression of $X^{(0)}(\epsilon_k,\epsilon_{k'},\epsilon_{k''})$ presented in the last subsection contains the umklapp sums because of an interference effect: X_1 and X_2 do not depend only on $\epsilon_k,\epsilon_{k'},\epsilon_{k''}$, but also on k,k',k''. Therefore these expressions are not suitable for the single-site approximation.

The $R=0$ approximation[42] is an often used single-site approximation. However, when applied to the matrix elements X_1 and X_2, the Fermi-liquid property $\tilde{\Lambda}_\sigma^{(i)}(0^+)=\Lambda_\sigma^{(i)}(0^+) - U\langle n_{i-\sigma}\rangle = 0$ is generally not satisfied. For that reason we extend the approximation as follows. The $R=0$ approximation implies a replacement of $f(\epsilon_{k_1\sigma})$ [or $f(\epsilon_{k_1'\sigma})$] by a representative value $\langle n_{i\sigma}\rangle_0$ in the umklapp sums of, e.g., Eq. (33). As an extension, we shall approximate the umklapp sum with respect to k_1 and k_1' by an average of two representative values leading to a single-site approximation. We call this approximation the two-point approximation. For example, we may take point $(k_1,k_1')=(k,k'')$ with a weight r_1, and $(k_1,k_1')=(-k'',-k)$ with a weight r_2 in the first sum of the RHS of Eq. (33), and point $(k_1,k_1')=(k,k')$ with a weight s_1 and $(k_1,k_1')=(k',k)$ with a weight s_2 in the second sum. Because $f(\epsilon_k)f(-\epsilon_k)=0$ and $f(\epsilon_k)^2=f(\epsilon_k)$ when the ground state, we end up with

$$X_1(\epsilon_k,\epsilon_{k'},\epsilon_{k''}) = -r_2[f(-\epsilon_k)f(\epsilon_{k''})+f(\epsilon_k)f(-\epsilon_{k''})]. \quad (35)$$

In the same way, we obtain

$$\begin{aligned} X_2(\epsilon_k,\epsilon_{k'},\epsilon_{k''}) &= \frac{1}{4}\{u_1[f(\epsilon_{k''})-f(\epsilon_{k'})]^2 - v_1[f(\epsilon_k)-f(-\epsilon_k)][f(\epsilon_{k''})-f(-\epsilon_{k''})] - v_2[f(-\epsilon_k)-f(\epsilon_{k''})]^2 \\ &\quad + w_1[f(\epsilon_k)-f(-\epsilon_k)][f(\epsilon_{k'})-f(-\epsilon_{k'})] + w_2[f(-\epsilon_k)-f(\epsilon_{k'})]^2\} \\ &\quad + \frac{1}{8}\{[f(\epsilon_k)-f(\epsilon_{k''})][f(-\epsilon_{k'})-f(\epsilon_{k'})]+[f(-\epsilon_k)-f(\epsilon_{k'})][f(-\epsilon_{k''})-f(\epsilon_{k''})]+[f(\epsilon_{k''})-f(\epsilon_{k'})][f(\epsilon_k)-f(-\epsilon_k)]\}. \end{aligned} \quad (36)$$

Substituting Eqs. (28) and (32) into Eqs. (15)–(17), and using X_1 and X_2 given by Eqs. (35) and (36), we obtain the screened memory function as

$$\overline{G}_0^{(i)}(z) = M^{(0)}(z - \tilde{\Sigma}(z)) + \frac{M^{(1)}(z - \tilde{\Sigma}(z), \tilde{\Sigma}(z))}{1 - R^{(i)}(z - \tilde{\Sigma}(z)) + \overline{L}_I^{(i)}(z)\hat{\Sigma}^{(2)}(z - \tilde{\Sigma}(z))}, \tag{37}$$

$$M^{(0)}(z) = \hat{\Sigma}^{(2)}(z) - \frac{\hat{\eta}}{1+\hat{\eta}^2} M_1^{(0)}(z) + \frac{\hat{\eta}^2}{1+\hat{\eta}^2} M_2^{(0)}(z), \tag{38}$$

$$M^{(1)}(z, \tilde{\Sigma}(z)) = -\tilde{\Sigma}(z)\tilde{M}^{(1)}(z) + U\overline{M}^{(1)}(z) - \overline{L}_I^{(i)}(z) M^{(0)}(z)\hat{\Sigma}^{(2)}(z), \tag{39}$$

$$\tilde{M}^{(1)}(z) = \tilde{M}_0^{(1)}(z) - \frac{\hat{\eta}}{1+\hat{\eta}^2}\tilde{M}_1^{(1)}(z) + \frac{\hat{\eta}^2}{1+\hat{\eta}^2}\tilde{M}_2^{(1)}(z), \tag{40}$$

$$\overline{M}^{(1)}(z) = -\frac{\hat{\eta}}{1+\hat{\eta}^2}\overline{M}_1^{(1)}(z) + \frac{\hat{\eta}^2}{1+\hat{\eta}^2}\overline{M}_2^{(1)}(z), \tag{41}$$

$$R^{(i)}(z) = -\tilde{\Sigma}(z)\int d\epsilon\, d\epsilon'\, d\epsilon''\rho(\epsilon)\rho(\epsilon')\rho(\epsilon'')[\hat{F}(z-\epsilon'+\epsilon'') + \hat{F}(z-\epsilon+\epsilon'') - \hat{F}(z-\epsilon-\epsilon')]. \tag{42}$$

Here $\hat{\eta} = \eta/4$. The functions $M_n^{(0)}(z)$ $(n=1,2)$ in Eq. (38) are given by $\hat{\Sigma}^{(2)}(z)$ [see Eq. (27)] in which $\chi(\epsilon,\epsilon',\epsilon'')$ has been replaced by $4X_1(\epsilon,\epsilon',\epsilon'')$ and $16X_2(\epsilon,\epsilon',\epsilon'')$, respectively. The $\tilde{M}_n^{(1)}(z)$ $(n=0,1,2)$ in Eq. (40) are defined by $\hat{\Sigma}^{(2)}(z)$ in which $\chi(\epsilon,\epsilon',\epsilon'')$ has been replaced by $\chi(\epsilon,\epsilon',\epsilon'')[\hat{F}(z-\epsilon'+\epsilon'')+\hat{F}(z-\epsilon+\epsilon'')-\hat{F}(z-\epsilon-\epsilon')]$, $4X_1(\epsilon,\epsilon',\epsilon'')[\hat{F}(z-\epsilon'+\epsilon'')+\hat{F}(z-\epsilon+\epsilon'')-\hat{F}(z-\epsilon-\epsilon')]$, and $16X_2(\epsilon,\epsilon',\epsilon'')[\hat{F}(z-\epsilon'+\epsilon'')+\hat{F}(z-\epsilon+\epsilon'')-\hat{F}(z-\epsilon-\epsilon')]$. In the same way, the $\overline{M}_n^{(1)}(z)$ $(n=1,2)$ in Eq. (41) are defined by $\hat{\Sigma}^{(2)}(z)$ in which $\chi(\epsilon,\epsilon',\epsilon'')$ has been replaced by $4X_1(\epsilon,\epsilon',\epsilon'')K(z,\epsilon',\epsilon'')$ and $16X_2(\epsilon,\epsilon',\epsilon'')K(z,\epsilon',\epsilon'')$, respectively. Here $\hat{F}(z)$ and $K(z,\epsilon',\epsilon'')$ are given by Eqs. (25) and (26).

C. Fermi-liquid condition and screened memory function

The two-point approximation has introduced several parameters as is seen from Eqs. (35) and (36). They are reduced by the Fermi-liquid condition $\tilde{\Lambda}^{(i)}(0^+)=0$. When we introduce a function $M(z,\tilde{\Sigma}(z))$ such that $\overline{G}_0^{(i)}(z) = M(z - \tilde{\Sigma}(z), \tilde{\Sigma}(z))$, this condition is expressed as $M(0^+,0)=0$. Substituting Eq. (37) into this equation, we obtain the following explicit Fermi-liquid conditions:

$$\hat{\Sigma}^{(2)}(0^+) = 0, \tag{43}$$

$$M_1^{(0)}(0^+) = \overline{M}_1^{(1)}(0^+) = 0, \tag{44}$$

$$M_2^{(0)}(0^+) = 0, \tag{45}$$

$$\overline{M}_2^{(1)}(0^+) = 0. \tag{46}$$

Equation (43) is automatically satisfied. Equation (44) leads to the condition $r_2=0$. This implies that $M_1^{(0)}(z) = \tilde{M}_1^{(1)}(z) = \overline{M}_1^{(1)}(z) = 0$. Equation (45) yields the following relation:

$$u_1 + v_1 - 2w_1 + w - 2v + \tfrac{3}{2} = 0. \tag{47}$$

Here we adopted a Gaussian DOS $\rho(\epsilon) = (1/\sqrt{\pi})\exp(-\epsilon^2)$, and $w = w_1 + w_2$ and $v = v_1 + v_2$. Finally, the condition (46) is equivalent to the following relation:

$$2v_1 - 2w_1 + v_2 - w_2 = 0. \tag{48}$$

We therefore obtain $\overline{M}_2^{(1)}(z)=0$.

Equations (47) and (48) show that one can express the five parameters u_1, v_1, v_2, w_1, and w_2 by means of three parameters u_1, v, and w, i.e., $v_1 = u_1 - 4v + 3w + 3/2$, $v_2 = -u_1 + 5v - 3w - 3/2$, $w_1 = u_1 - 3v + 2w + 3/2$, $w_2 = -u_1 + 3v - w - 3/2$. Making use of these relations and the results $M_1^{(0)}(z) = \tilde{M}_1^{(1)}(z) = \overline{M}_1^{(1)}(z) = 0$ as well as $\overline{M}_2^{(1)}(z)=0$, we obtain the following final expression for the screened memory function in the two-point approximation:

$$\overline{G}_0^{(i)}(z) = \hat{\Sigma}^{(2)}(z - \tilde{\Sigma}(z)) + \frac{M^{(1)}(z - \tilde{\Sigma}(z), \tilde{\Sigma}(z))}{1 - R^{(i)}(z - \tilde{\Sigma}(z)) + \overline{L}_I^{(i)}(z)\hat{\Sigma}^{(2)}(z - \tilde{\Sigma}(z))}, \tag{49}$$

$$M^{(1)}(z, \tilde{\Sigma}(z)) = -\tilde{\Sigma}(z)\tilde{M}^{(1)}(z) - \overline{L}_I^{(i)}(z) M^{(0)}(z)\hat{\Sigma}^{(2)}(z), \tag{50}$$

$$M^{(0)}(z) = \hat{\Sigma}^{(2)}(z) + 8[u_1 - 2(v-w)]\frac{\hat{\eta}^2}{1+\hat{\eta}^2}\hat{\Sigma}^{(2)}(z), \tag{51}$$

$$\tilde{M}^{(1)}(z) = \tilde{M}_0^{(1)}(z) + \frac{\hat{\eta}^2}{1+\hat{\eta}^2}\tilde{M}_2^{(1)}(z), \tag{52}$$

$$\tilde{M}_2^{(1)}(z) = 4(u_1 - 1)\tilde{m}_1(z) + [-4(v-w) + 2]\tilde{m}_2(z), \tag{53}$$

$$\tilde{m}_1(z) = \int \frac{d\epsilon\, d\epsilon'\, d\epsilon''\rho(\epsilon)\rho(\epsilon')\rho(\epsilon'')}{z - \epsilon - \epsilon' + \epsilon''}(\{[f(\epsilon'') - f(\epsilon')]^2 + 2[f(\epsilon') - f(-\epsilon)]^2\}\hat{F}(z - \epsilon' + \epsilon'') - [f(\epsilon') - f(-\epsilon)]^2\hat{F}(z - \epsilon - \epsilon') - [f(\epsilon'') - f(-\epsilon)]^2\hat{F}(z - \epsilon + \epsilon'')), \tag{54}$$

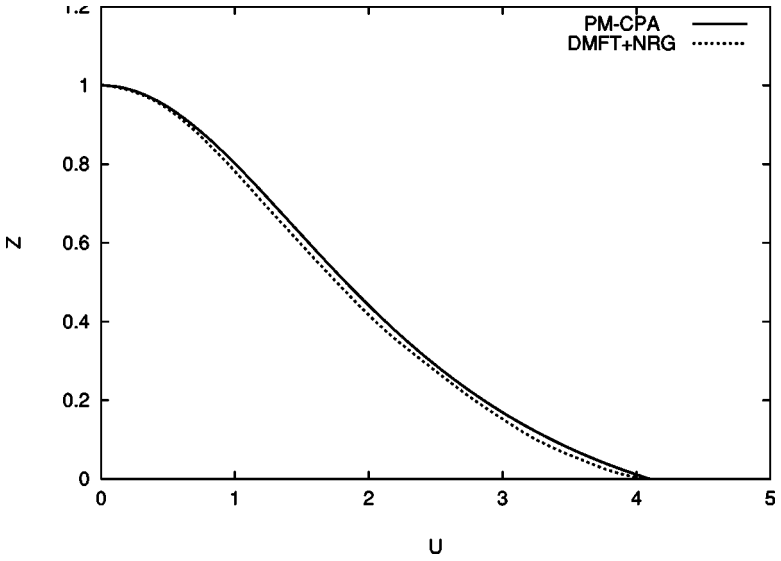

FIG. 1. Quasiparticle weight vs Coulomb interaction curves in the PM-CPA (solid curve) and the DMFT + NRG (dotted curve) (Ref. 43) at the ground state. A half-filled band on a hypercubic lattice in infinite dimensions is assumed. The energy unit is chosen so that the second moment of the noninteracting density of states becomes $1/2$.

$$\tilde{m}_2(z) = \int \frac{d\epsilon\, d\epsilon'\, d\epsilon'' \rho(\epsilon)\rho(\epsilon')\rho(\epsilon'')}{z-\epsilon-\epsilon'+\epsilon''} (\{[f(\epsilon'')-f(\epsilon')]^2 + 2[f(\epsilon'')-f(-\epsilon')]^2 + 6[f(\epsilon')-f(-\epsilon)]^2\} \times \hat{F}(z-\epsilon'+\epsilon'') - 3[f(\epsilon')-f(-\epsilon)]^2 \hat{F}(z-\epsilon-\epsilon') - 3[f(\epsilon'')-f(-\epsilon)]^2 \hat{F}(z-\epsilon+\epsilon'')). \quad (55)$$

Here the lowest moment of $\overline{G_0^{(i)}}(z)$ does not necessarily reproduce the exact value $\langle n_{i-\sigma}\rangle(1-\langle n_{i-\sigma}\rangle)=1/4$. To improve this point, we have introduced a constant prefactor into the first term (i.e., $[\overline{G_0^{(i)}}(z)]_0$) on the RHS of Eq. (49), and determined it so that the correct moment is reproduced. Note that as a result there is no correlation correction to the first term (the RPT-0). The local correlations modify only the second term via $M^{(1)}(z,\tilde{\Sigma}(z))$. Equations (11) and (49)–(55), and the CPA equations (6) determine self-consistently the single-particle excitation spectrum of the system.

The self-consistent equation for the determination of the critical Coulomb interaction U_{c1}(gap) for a gap formation is obtained by using the previous result[40] as follows:

$$U = 4\sqrt{c_2^{(0)} + d_3^{(1)}}, \quad (56)$$

$$d_3^{(1)} = d_{30}^{(1)} + \frac{\hat{\eta}^2}{1+\hat{\eta}^2} d_{32}^{(1)}. \quad (57)$$

Here $c_2^{(0)}=3/8+3/2\pi$, $d_{30}^{(1)}=1/4$, and $d_{32}^{(1)}=2u_1-4(1-3/\pi)\times(v-w)-6/\pi$ for the Gaussian DOS.

The critical Coulomb interaction $U_{c2}(m^*=\infty)$ for the divergence of the effective mass is determined from the equation[40]

$$U = \frac{1}{\sqrt{-\partial\hat{\Sigma}^{(2)}(0^+)/\partial z - \tilde{M}^{(1)}(0^+)}}. \quad (58)$$

Here $\partial\hat{\Sigma}^{(2)}(0^+)/\partial z=-0.1572$ for a Gaussian DOS. Furthermore, $\tilde{M}^{(1)}(0^+)$ is obtained from Eq. (52) with $\tilde{m}_1(0^+)=0.3145$ and $\tilde{m}_2(0^+)=0.1442$. The quasiparticle weight Z is obtained from the following formula:[40]

$$Z = \frac{1-(U/U_{c2})^2}{1+(U/U_2)^2}. \quad (59)$$

Here U_{c2} is defined by the RHS of Eq. (58), and $U_2=1/\sqrt{\tilde{M}^{(1)}(0^+)}$.

IV. NUMERICAL RESULTS

The memory function presented in the last section allows us to investigate the correlation effects on the excitation spectrum. We performed numerical calculations of the excitation spectrum for a half-filled band on a hypercubic lattice in infinite dimensions. In this case, the DOS for the noninteracting system is given by the Gaussian function $\rho(\epsilon)=(1/\sqrt{\pi})\exp(-\epsilon^2)$. The present theory contains two parameters u_1 and $v-w$. These parameters should take the values $0\lesssim u_1\lesssim 1$ and $v-w\sim 0$ for physical reasons. We choose the parameters here so that the calculated $U_{c2}(m^*=\infty)$ yields the best value 4.10 as obtained by the numerical renormalization group approach[43] (NRG) and that the condition $U_{c1}(\text{gap})<U_{c2}(m^*=\infty)$ is satisfied. The latter requires the inequality $v-w<-0.2625$. Taking into account the physical condition $v-w\sim 0$, we choose the values $u_1=0.715$ and $v-w=-0.30$. These values yield the critical Coulomb interaction $U_{c1}(\text{gap})=4.09$. In the numerical calculations, we adopted the Fourier representation of the memory function. When $|\tilde{\Sigma}(z)|\gg 1$, the moment expansion to the memory function is useful to avoid numerical problems.

The quasiparticle weight vs U is calculated from Eq. (59). With the above parameters the curve obtained by the NRG approach is reproduced very well (see Fig. 1). Although there is some ambiguity for the choice of $v-w$ between -0.5 and -0.2, the calculated DOSs are not sensitive to a particular choice even in the intermediate Coulomb interaction regime (see Fig. 2).

Figure 3 shows the calculated DOS for various values of the Coulomb interaction U. For $U\lesssim 2.0$, the correlation cor-

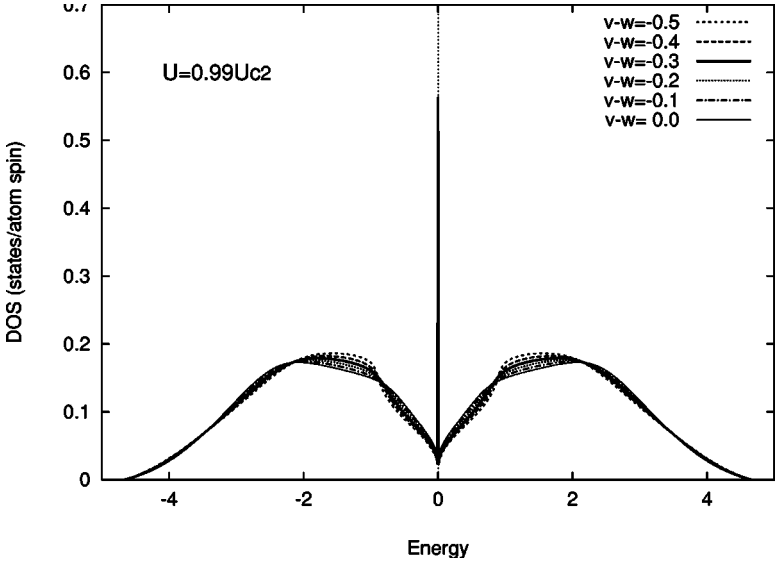

FIG. 2. Densities of states when the parameter $v-w$ is varied under the condition $U_{c2}(m^*=\infty)=4.10$. The Coulomb interaction U is fixed to be $0.99U_{c2}(m^*=\infty)$.

rections to the static average in the DOS are negligible. For $U\simeq 3.0$, the weight around $\omega=\pm 1.0$ is enhanced due to correlations. When $U=3.5$, we find a dip around $\omega=0$ due to correlations and the shoulders at $\omega\approx\pm 2.5$ are reduced, showing the formation of the upper and lower Hubbard bands. Between $U=3.7$ and 4.1, the Fermi-liquid state persists in the present correlation calculations, while in the Hartree-Fock approximation a non-Fermi-liquid state without a gap appears between $U=3.7$ and $U=4.2$. In our previous paper, we described the spectrum in this region by means of the first term (i.e., the RPT-0 term) on the RHS of Eq. (49) introducing a cutoff factor $q=0$ into the second term. For $U\geqslant 4.1$ an insulator state with a finite gap appears in the present approach.

Figure 4 shows more precisely the formation of the upper and lower Hubbard bands due to correlations. The quasigap around $\omega=0$ is less pronounced than that obtained by the NRG calculations. The weight of the peaks at $\omega=\pm U/2$ is considerably lower than the one in the NRG. This is partly attributed to the weak coupling approximation (28) which neglects the correlation effects on the higher-order terms, and partly to the local ansatz (29) which is less suitable for the strong Coulomb interaction regime.

A characteristic feature of the spectrum for strong Coulomb interactions is that the upper and the lower Hubbard bands for high-energy excitations are mainly described by the first term in Eq. (49), i.e., the RPT-0 with the use of the Hartree-Fock wave function as shown in Fig. 5. This feature justifies the cutoff parameter $q=1$ for $U<U_{c2}(m^*=\infty)$ and $q=0$ for $U>U_{c2}(m^*=\infty)$, introduced into the second term of Eq. (37) in our previous paper.[40] This was done in order to simulate within the Hartree-Fock approximation scheme effectively the correlation effects in the strong Coulomb interaction regime.

The lattice spectral function $\rho_k(\omega)$ is given by $-\pi^{-1}\,\mathrm{Im}\{[z-\epsilon_k-\tilde{\Sigma}(z)]^{-1}\}$ for the half-filled band. Its momentum dependence is given by the band energy ϵ_k because the self-energy is momentum independent in infinite dimensions. Figure 6 shows the spectral functions $\rho(\epsilon_k,\omega)$ calculated at $U=3.5$ for different ϵ_k. Note that $\epsilon_k=-\infty$ at the Γ point

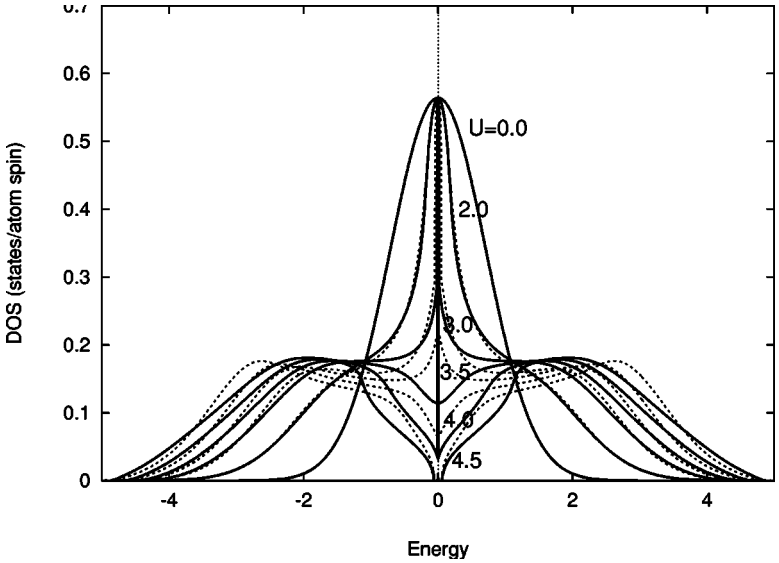

FIG. 3. DOS for various Coulomb interactions (U). Solid curves (dotted curves) are calculated from the matrix elements with (without) electron correlations.

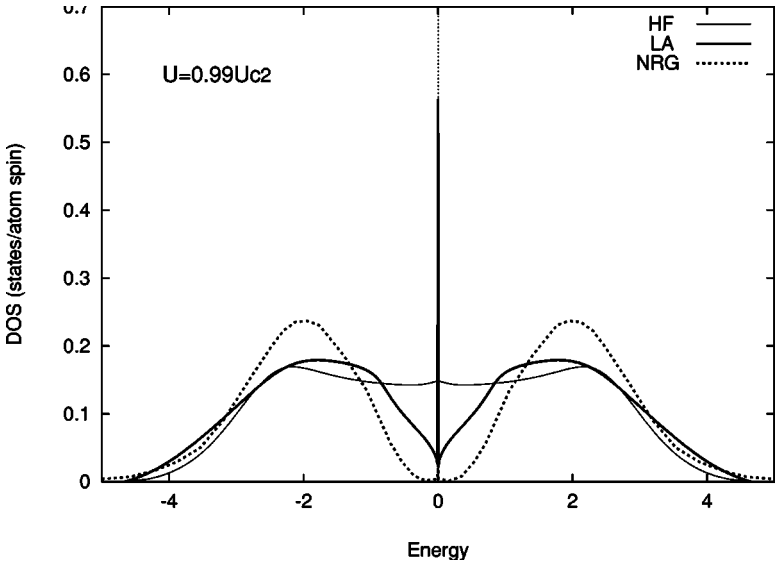

FIG. 4. DOS near the critical Coulomb interaction in various methods: the PM-CPA in the Hartree-Fock approximation scheme (thin solid curve), the PM-CPA with use of the Gutzwiller-type wave function (solid curve), and the DMFT with use of the NRG (dotted curve).

$(0,\ldots,0)$ and $\epsilon_k=\infty$ at the R point $(\pi,\ldots,\pi)$. Moreover, $\rho(-\epsilon_k,\omega)=\rho(\epsilon_k,-\omega)$ for a half-filled band on the hypercubic lattice. For large $|\epsilon_k|$, the spectrum shows a single peak because correlations are weak in that limit. When $|\epsilon_k|\sim U$, two peaks appear due to local excitations around $\epsilon_0-\mu+\epsilon_k$ and $\epsilon_0-\mu+\epsilon_k+U$. When $|\epsilon_k|\sim 0$, we find a low-energy quasiparticle peak at $\omega\sim 0$ as well as Mott-Hubbard peaks at $|\omega|\sim U/2$. The effect of electron correlations on the static matrix elements enhances the Mott-Hubbard type incoherent peaks, hence reducing the states near the Fermi level.

V. SUMMARY

We have investigated in the present paper the effects of correlation on the static matrix elements in the memory function of the projection operator method CPA. These matrix elements were calculated by means of a Gutzwiller-type variational wave function within a single-site approximation. By making use of the weak-scattering approximation that linearizes the correlation effects, we obtained an explicit form of the memory function.

The $R=0$ approximation to the matrix elements obtained from the Gutzwiller-type local ansatz is not consistent with a Fermi-liquid description of the excitation spectrum. We therefore adopted a two-point approximation for the evaluation of the umklapp sums in the memory function. The two-point approximation introduces additional parameters of weighting factors. The Fermi-liquid condition reduces the number of parameters. Remaining are two parameters which are directly related to the critical Coulomb interactions U_{c1}(gap) and $U_{c2}(m^*=\infty)$. In this sense, the present theory does not determine these critical Coulomb interactions. Nevertheless, one can investigate the correlation effects on other quantities by taking reasonable values for the two parameters. The changes of the DOS are very small when the parameters are varied under the condition that $U_{c2}(m^*=\infty)=4.10$ (the NRG value).

The obtained self-energy shows a simple structure. There is no local correlation effect to the zeroth order term in the

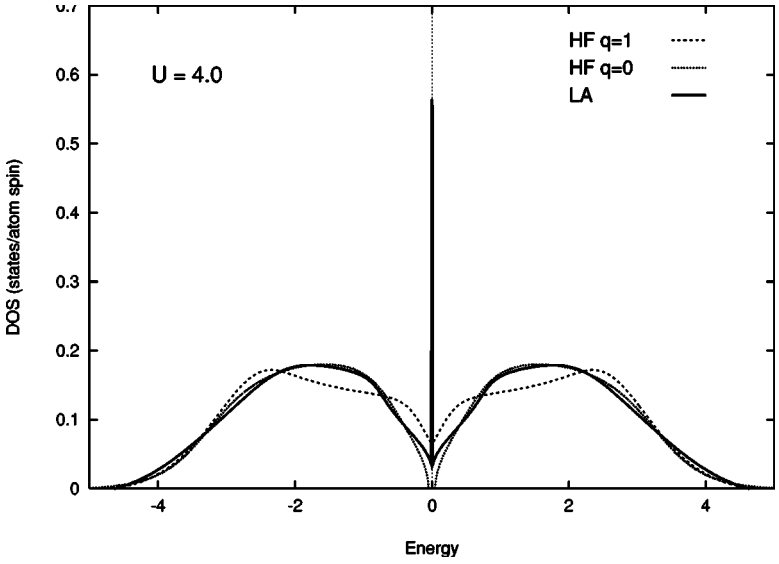

FIG. 5. DOS calculated by using (a) the Hartree-Fock approximation plus a cutoff $q=1$ (dashed curve), (b) the Hartree-Fock approximation and a cutoff $q=0$ (dotted curve), and (c) the present scheme based on the local ansatz wave function (solid curve). The Coulomb interaction parameter is kept fixed $U=4.0$.

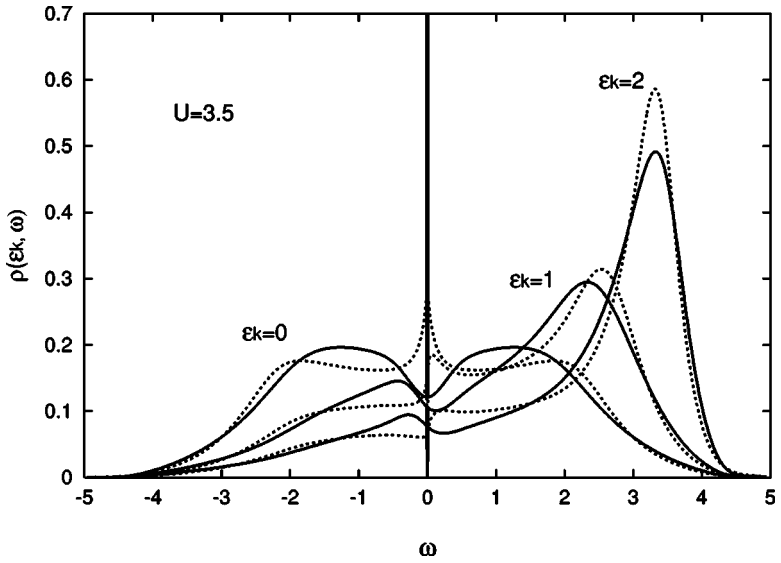

FIG. 6. Spectral functions for various kinetic energies $\epsilon_k = 0,1,2$, including the effects of electron correlations on the static matrix elements (solid curves) and without correlations (dotted curves).

expansion of the screened memory function. The local correlation term appears only via the $\tilde{\Sigma}$-linear term in the first order expansion term. We have shown that the local correlations on the static matrix elements improve the excitation spectrum in the intermediate Coulomb interaction regime. The upper and lower Hubbard bands are developed by the correlation corrections near the critical Coulomb interactions. Furthermore these bands are well described by the zeroth order term in the screened memory function. As the result, the effects of electron correlations on the static averages justify to use instead a Hartree-Fock approximation scheme with a cutoff function, as proposed in our previous paper.[40]

The present theory contains two problems which should be improved in the future. First, we introduced phenomenological parameters to describe the Fermi-liquid property of the system. This originated in the difficulty that a simple single-site approximation to the static averages with respect to the Gutzwiller-type local ansatz variational wave function is not consistent with a Fermi-liquid behavior of the single-particle excitation spectrum. To remove the difficulty, one has to improve the variational wave function so as to describe the low-energy excitations due to Coulomb interactions.

Second, we adopted a weak-scattering approximation in the calculations of the static matrix elements. This implies neglecting the correlation effects on the higher-order matrix elements $\Delta_\sigma(z, \epsilon_k, \epsilon_{k'}, \epsilon_{k''})$ in the expansion of the screened memory function. When the Coulomb interaction U is increased, electrons are localized to avoid a double occupancy of a site, so that the operator space used by the correlated electrons is reduced from $\{a^\dagger_{k\sigma}\delta(a^\dagger_{k'-\sigma}a_{k''-\sigma})\}$ to $\{A^\dagger_{i\sigma}\}$. This implies that $\Delta_\sigma(z, \epsilon_k, \epsilon_{k'}, \epsilon_{k''})$ vanishes in the strongly correlated regime, i.e., $\Delta_\sigma(z, \epsilon_k, \epsilon_{k'}, \epsilon_{k''}) \to 0$ because the matrix elements $(\tilde{\mathbf{L}}^{(i)}_{IQ})_{k_1 k_1' k_1'' \sigma k k' k'' \sigma} \to 0$ when $U \to \infty$ [see Eq. (19)]. Such a screening effect on the higher-order terms should further localize the electrons. We therefore expect that in the intermediate Coulomb interaction regime the higher-order corrections should enhance the peaks of the Hubbard bands at $\omega = \pm U$. Solving these problems is left for future investigations toward a quantitative and analytic description of the excitation spectrum.

[1] See, for example, P. Fulde, *Electron Correlations in Molecules and Solids* (Springer, Berlin, 1995), Chap. 11.
[2] J. Hubbard, Proc. R. Soc. London, Ser. A **276**, 238 (1963).
[3] J. Hubbard, Proc. R. Soc. London, Ser. A **281**, 401 (1964).
[4] P. Soven, Phys. Rev. **156**, 809 (1967); **178**, 1136 (1969).
[5] D. W. Taylor, Phys. Rev. **156**, 1017 (1967).
[6] B. Velický, S. Kirkpatrick, and H. Ehrenreich, Phys. Rev. **175**, 747 (1968).
[7] R. J. Elliott, J. A. Krumhansl, and P. L. Leath, Rev. Mod. Phys. **46**, 465 (1974).
[8] H. Ehrenreich and L. M. Schwartz, in *Solid State Physics*, edited by H. Ehrenreich, F. Seitz, and D. Turnbull (Academic, New York, 1980), Vol. 30.
[9] H. Shiba, Prog. Theor. Phys. **46**, 77 (1971).
[10] M. C. Gutzwiller, Phys. Rev. Lett. **10**, 159 (1963).
[11] M. C. Gutzwiller, Phys. Rev. **134**, A923 (1964); **137**, A1726 (1965).
[12] W. F. Brinkman and T. M. Rice, Phys. Rev. B **2**, 4302 (1970).
[13] W. Metzner and D. Vollhardt, Phys. Rev. Lett. **62**, 324 (1989).
[14] E. Müller-Hartmann, Z. Phys. B: Condens. Matter **74**, 507 (1989).
[15] U. Brandt and C. Mielsch, Z. Phys. B: Condens. Matter **75**, 365 (1989); **79**, 295 (1991); **82**, 37 (1991).
[16] V. Janis, Phys. Rev. B **40**, 11 331 (1989); Z. Phys. B: Condens. Matter **83**, 227 (1991).
[17] M. Jarrell, Phys. Rev. Lett. **69**, 168 (1992); M. Jarrell and H. R. Krishnamurthy, Phys. Rev. B **63** 125102 (2001).
[18] A. Georges and G. Kotliar, Phys. Rev. B **45**, 6479 (1992).
[19] See, for example, A. Georges, G. Kotliar, W. Krauth, and M. J. Rosenberg, Rev. Mod. Phys. **68**, 13 (1996).

[20] M. Cyrot, J. Phys. (Paris) **33**, 25 (1972).
[21] J. Hubbard, Phys. Rev. B **19**, 2626 (1979); **20**, 4584 (1979); **23**, 5974 (1981).
[22] H. Hasegawa, J. Phys. Soc. Jpn. **46**, 1504 (1979); **49**, 178 (1980).
[23] J. Hubbard, Phys. Rev. Lett. **3**, 77 (1959).
[24] R. L. Stratonovich, Dokl. Akad. Nauk SSSR **115**, 1097 (1958) [Sov. Phys. Dokl. **2**, 416 (1958)].
[25] S. Q. Wang, W. E. Evanson, and J. R. Schrieffer, Phys. Rev. Lett. **23**, 92 (1969); J. Appl. Phys. **41**, 1199 (1970).
[26] G. Morandi, E. Galleani D'Agliano, F. Napoli, and C. F. Ratto, Adv. Phys. **23**, 867 (1974).
[27] Y. Kakehashi and P. Fulde, Phys. Rev. B **32**, 1595 (1985).
[28] Y. Kakehashi, Phys. Rev. B **45**, 7196 (1992); J. Magn. Magn. Mater. **104-107**, 677 (1992).
[29] Y. Kakehashi, Phys. Rev. B **65**, 184420 (2002).
[30] S. Hirooka and M. Shimizu, J. Phys. Soc. Jpn. **43**, 70 (1977).
[31] Y. Kakehashi, Phys. Rev. B **66**, 104428 (2002).
[32] H. Mori, Prog. Theor. Phys. **33**, 423 (1965).
[33] R. Zwanzig, *Lectures in Theoretical Physics* (Interscience, New York, 1961), Vol. 3.
[34] W. D. Lukas and P. Fulde, Z. Phys. B: Condens. Matter **48**, 113 (1982).
[35] K. W. Becker and W. Brenig, Z. Phys. B: Condens. Matter **79**, 195 (1990).
[36] P. Unger and P. Fulde, Phys. Rev. B **48**, 16 607 (1993).
[37] P. Unger, J. Igarashi, and P. Fulde, Phys. Rev. B **50**, 10 485 (1994).
[38] P. Fulde, Adv. Phys. **51**, 909 (2002).
[39] H. Stoll, Phys. Rev. B **46**, 6700 (1992); Chem. Phys. Lett. **191**, 548 (1992).
[40] Y. Kakehashi and P. Fulde, Phys. Rev. B **69**, 045101 (2004).
[41] G. Stollhoff and P. Fulde, Z. Phys. B **29**, 231 (1978); J. Chem. Phys. **73**, 4548 (1980).
[42] G. Treglia, F. Ducastelle, and D. Spanjaard, Phys. Rev. B **21**, 3729 (1980).
[43] R. Bulla, Phys. Rev. Lett. **83**, 136 (1999).